Nuclear Instruments and Methods in Physics Research B xxx (2017) xxx–xxx

Contents lists available at ScienceDirect

Nuclear Instruments and Methods in Physics Research B

journal homepage: www.elsevier.com/locate/nimb

Water fragmentation induced by ion impact: Fragment-ion-energy determination at different Z_P/v regimes

N.D. Cariatore [a], S. Otranto [a], W. Wolff [b,*], H. Luna [b], F. Turco [c], D. Fregenal [c], G. Bernardi [c], S. Suárez [c], R. Schuch [d]

[a] IFISUR, Universidad Nacional del Sur, CONICET, Departamento de Física, Bahía Blanca, Argentina
[b] Instituto de Física, Universidade Federal do Rio de Janeiro, Caixa Postal 68528, Rio de Janeiro 21945-970, RJ, Brazil
[c] Centro Atómico Bariloche, Bustillo 9500, San Carlos de Bariloche, Río Negro, Argentina
[d] Department of Physics, Stockholm University, Alba Nova University Center, SE-106 91 Stockholm, Sweden

ARTICLE INFO

Article history:
Received 10 November 2016
Accepted 30 April 2017
Available online xxxx

Keywords:
Ion-molecule collision
Multiple ionization
Fragmentation
Monte Carlo simulation

ABSTRACT

This work focuses on the energy distributions of positive water ionic fragments produced by ion impact at MeV impact energies. An improved Coulomb explosion model coupled to a classical trajectory Monte Carlo simulation is used to provide energy centroids of the fragments for the dissociation channels resulting from the removal of two to five electrons from the water molecule. This model explicitly includes the post-collisional interaction of the projectile with the resulting ionic fragments affecting their kinetic energy release spectra especially at low impact energies. Theoretical data are benchmarked against recent data collected for 220 keV $Xe^{22+} + H_2O$ collisions which corresponds to a large Z_P/v collision parameter. To extend our tests to the low Z_P/v regime, fragment species as a function of emission energy and time-of-flight were recorded in 3 MeV Li^{3+} collisions by using an electrostatic spectrometer and a time-of-flight mass spectrometer, respectively. Present experimental data reveals the existence of multiple-ionization processes leading to charge state up to 4+.

1. Introduction

Recent estimates for cancer decease indicate that one over seven deaths worldwide are due to cancer and that about 14 million new cases of cancer are diagnosed each year [1]. In this context, and based on the complexity of the problem, different lines of investigation are pushed from several fields and will lead to more effective interdisciplinary approaches in a near future. From the physical point of view, considerable efforts have been made to learn on the irradiation of tumors by high-energy protons and carbon ions to make possible the ion-beam therapy technique.

In this sense, one of the most demanding problems nowadays is the precise determination of the energy deposition to reduce the irradiation of healthy tissue or organs. One of the advantages of ion-beam therapy, compared to other techniques such as radiotherapy, is that the energy deposition is mostly localized around the denominated Bragg peak [1]. However, the determination of such peak in an environment as complex as the human body can only be achieved by means of numerical simulations of the irradiation process. A clear challenge faced by the atomic and molecular collisions community is to provide the physical grounds for the irradiation process (cross sections, probabilities, energy distributions of resulting fragments in molecular ion dissociation processes etc.) to improve the outcomes of the energy deposition simulators currently under use.

In this work, we consider the water molecule as the archetypal biological target and focus our attention on the determination of the energy distributions of the resulting positive ionic fragments following collisions with ions in the keV-MeV impact energy range which lead to multiple electron removal. In section 2, we describe the theoretical model employed, which is based on a Coulomb Explosion model coupled to n-electron classical trajectory Monte Carlo (nCTMC) simulations. In section 3 we briefly describe the experimental procedure, with focus on the determination of the total ion-fragments energy distributions. In section 4 the results are shown with emphasis on the similarities and differences observed with data obtained by other laboratories at keV/u impact energies. Relative yields of the fragmentation channels measured at the MeV energy range are reported giving estimates of which dissociative channel(s) dominates the total multiple ionization. In

* Corresponding author.
E-mail address: wania@if.ufrj.br (W. Wolff).

http://dx.doi.org/10.1016/j.nimb.2017.04.096
0168-583X/

section 5 conclusions and outlook are presented. Atomic units will be used throughout this work unless otherwise stated.

2. Theoretical method

The simple Coulomb Explosion model (CE) has been widely used for decades to describe the fragments dynamics in strong mutual repulsions. While many studies incorporate the standard assumption that molecular fragmentation takes place free from any perturbation due to the projectile, experimental studies performed more than a decade ago suggested that the kinetic energy release (KER) of fragments might not be unique as suggested by the CE model [2]. To illustrate this point, we mention the CO fragmentation results by Tarisien et al. [3] who observed that the resulting C^+ and O^+ fragments following charge exchange processes in O^{7+} + CO collisions at low impact energies led to energy shifts in the KER lines towards higher values when the molecule was aligned with the projectile beam direction [2,3]. This effect was originally predicted by Wood and Olson in 1999 in their CTMC study of the double ionization of H_2 by Xe^{54+} ions [4].

Now back to the topic of interest for this article, i.e. the fragmentation of the H_2O molecule by ion impact, we note that Pešic et al. [5] recently studied 220 keV Xe^{22+} + H_2O collisions which led to different fragmentation channels. Their experimental data was contrasted against CE simulations which explicitly incorporated the post-collisional interaction (PCI) between the emitted fragments and the receding projectile [5]. The projectile distance to the target used to initialize the CE was set by considering the capture distances provided by the classical over-barrier model [6,7]. The angular distribution of the KER of the resulting protons showed an anisotropy that became significant for protons emitted from the dissociation of multiply charged molecular ions.

In this work, we perform a theoretical study of the kinetic-energy spectra of ionic fragments by coupling a CE model with a n-body classical trajectory Monte Carlo (nCTMC) simulation. In this sense, the nCTMC model is used to develop a non-arbitrary criterion to determine, for each multiple capture and/or ionization event, the geometrical configuration of the collision system to be used to initialize the CE dynamics. In the present nCTMC model the water molecule is represented by a single center model in which eight electrons are sorted with sequential binding energies. This simplification is supported by the fact that self-consistent-field (SCF) wave-functions for the molecular orbitals of the H_2O molecule can be built in terms of an expansion of Slater orbitals upon the oxygen nucleus [8]. The interaction between the electrons and the dominant element of the molecule (oxygen) is represented by the parameterization provided by Garvey [9]

$$V(r) = \frac{(N-1)[1-\Omega(r)] - Z}{r} \tag{1}$$

$$\Omega(r) = \left[\left(\frac{\eta}{\xi}\right)(e^{\xi r} - 1) + 1\right]^{-1} \tag{2}$$

The corresponding parameters are Z = 8, N = 8, ξ = 1.36, η = 2.41. According to this potential, the target electrons see a charge +8 when they are near the oxygen nucleus, while they experience the asymptotic charge +1 at large distances.

In the present nCTMC simulation for each trajectory the position of the projectile-target saddle potential is tracked at all times. Each electron, removed from the target, is considered released from the target at the precise instant that it crosses the saddle structure for the last time, irreversibly leaving the target region. In Fig. 1 we show a schematic view of the potential surface for a +10 projectile approaching an O^+ ion. Saddle point crossings are identified in the simulation by contrasting at each time-step the

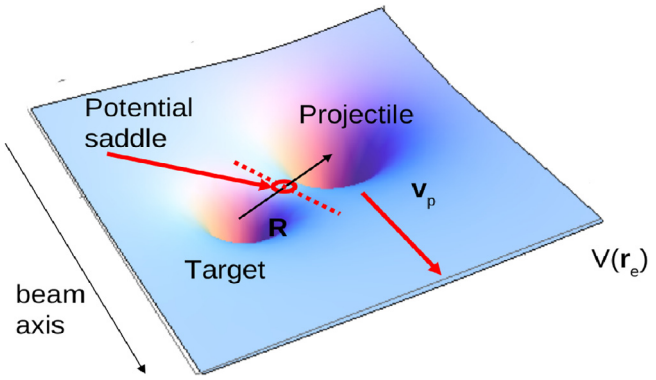

Fig. 1. Schematic view of the potential surface (V_{target} (r) + $V_{projectile}$(r)) for a +10 projectile impinging on O^+. Electron saddle crossings are determined by comparing $\mathbf{r}_{e^-}\cdots\mathbf{R}$ vs $\mathbf{r}_{saddle}$ at each time step of the nCTMC simulation.

projection of the electron-target position vector in the internuclear direction, i.e. $\mathbf{r}_{e^-}\cdots\mathbf{R}$ with the saddle position $\mathbf{r}_{saddle}$. The position and momentum of the projectile are recorded whenever an electron crosses the potential saddle leaving the target region.

In a second stage, a Coulomb explosion (CE) simulation proceeds. In this CE model the ionic fragments are explicitly considered and assumed to be at rest, still under the bonding length and angle of the neutral H_2O molecule. Furthermore, the H_2O molecule is assumed to be randomly oriented. The CE model is fed event by event with the positions and momenta of the projectile and target nucleus center of mass recorded at the instant the last ionized or captured electron crossed the potential saddle. The Coulomb explosion is then simulated by numerically solving Hamilton's equations for all ionic fragments plus the projectile. The total number of events recorded for n-electron capture or ionization, are used for each of those fragmentation channels corresponding to n-electron removal.

The main advantage of the present combined model, hereafter referred to as CE-CTMC, is that the Coulomb explosion dynamics are initialized considering the projectile's position and momentum at the time that the n-electron removal (via ionization, charge-exchange, or transfer-ionization mechanisms) takes place. Since such removal can be reached either in the incoming or outgoing phases of the projectile trajectory, CTMC provides a non-arbitrary route to initialize our CE model with PCI over a wide energy range. To further illustrate this point, in Fig. 2 we show histograms for the projectile position in the beam direction at the exact instant in which the saddle point is crossed by the last ionized or captured electron leading to multiple-electron removal ($z_{last\text{-}cross}$). In Fig. 2a we consider the collision system explored by Pešic (220 keV Xe^{22+} + H_2O) while in Fig. 2b we concentrate on the collision system experimentally explored in this work (3 MeV Li^{3+} + H_2O). These two cases provide complementary scenarios for the role of the projectile in a multiple-electron removal process which we now analyze in terms of Z_P/v, being Z_P the projectile charge and v the projectile velocity. Despite the fact, that in both cases the multiple-ionization is prone to take place once the projectile has surpassed the target, for low Z_P/v the histogram peaks around $z_{last\text{-}cross}$ = 0 and the influence of the projectile is inferred from the asymmetry of the structure towards the forward direction. In contrast, as Z_P/v increases the multiple-electron removal mostly takes place once the projectile has already surpassed the target ($z_{last\text{-}cross}$ > 0), highlighting that the explicit inclusion of the PCI with the projectile turns mandatory.

One of the most difficult fragmentation channels to describe by a CE model is $H_2O \rightarrow H^+ + OH^+$. As it has already been pointed out by Siegmann et al. [10], the unrealistic approximation of OH^+ by

Please cite this article in press as: N.D. Cariatore et al., Water fragmentation induced by ion impact: Fragment-ion-energy determination at different Z_P/v regimes, Nucl. Instr. Meth. B (2017), http://dx.doi.org/10.1016/j.nimb.2017.04.096

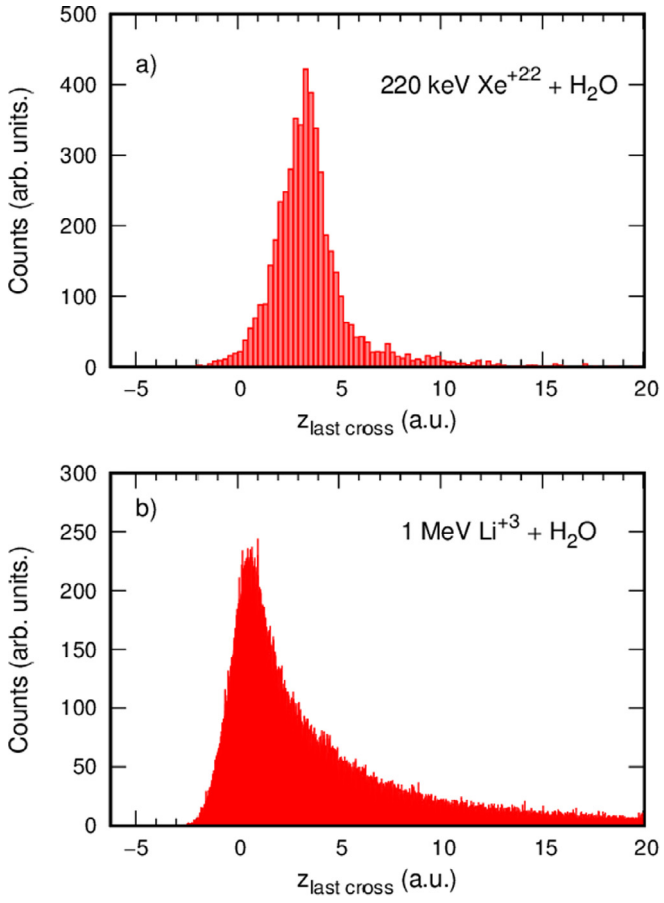

Fig. 2. nCTMC histograms for the projectile position along the beam axis at the instant the last electron saddle crossing characterizing a multiple-electron removal event takes place (z_last crossing). (a) 220 keV Xe^{22+} + H_2O. (b) 3 MeV Li^{3+} + H_2O.

a point charge located somewhere between the H and O nuclei leads to proton energies between 9 and 15 eV, which are larger than those measured by different laboratories which encompassed the range 4–7 eV. The incorporation of fractional charges [11,12] provides in principle a route to diminish the asymptotic proton energies. Preliminary tests did not lead us to the expected energy range. In fact, this fragmentation channel can be reached in principle via three possible mechanisms: (i) direct double ionization, which leads to an asymptotic proton energy of 6.8–7.1 eV [10,13]; (ii) resonant capture or inner-shell ionization followed by Auger deexcitation (asymptotic proton energy of about 4.6 eV) [13]; and (iii) single ionization or capture followed by electron excitation to autoionizing states of (OH), which then decay to $(OH)^+$ (kinetic-energy release of about 2–6 eV) [14].

Our first step towards a more detailed description of these fragmentation mechanisms has been the exploration of functional forms for the inter-fragment potentials that would physically fit and bring proton energies into agreement with the data. In this sense, two semi-empirical models have been employed at this stage which will be refined in future studies. For mechanism (i) we considered that the proton interacts with the $(OH)^+$ complex via a Coulomb interaction seeing an effective charge at short distances which via exponential factors evolves into a +1 charge at large distances. Mechanisms (ii) and (iii), on the other hand, rely on the fact that they originate in a single ionization or capture process. Hence, an $\propto r^{-2}$ dipole-type potential, which provides a rough approximation for a neutral environment, is used and switched into the same asymptotic Coulombic description of mechanism (i) by means of time-dependent exponential factors, $\exp(-\lambda t)$. The timescale for switching has been arbitrarily set to 5×10^{-15} s, which is typical for molecular rearrangements. In the following discussion, we refer to channels (ii) or (iii) as $H^+ + (OH)^*$, provided they lead to similar proton energies.

3. Experimental method

The experimental setup used in this work was previously explained in Ref. [15] and only minor descriptions will be given here. Briefly, a 3 MeV Li^{3+} beam was obtained from the 1.7 MV Pelletron accelerator facility of the Centro Atómico Bariloche. The beam was subsequently selected in mass, energy and charge state by a switching magnet and directed towards the projectile-target collision beam line. The beam current of all projectile species used in this work is measured at the end of the beam line by a biased Faraday cup, with typical beam currents of 10–70 nA. The water target is stored in a glass vessel and degassed by several thaw-pump cycles, eliminating mostly air contaminants. It is sublimated at room temperature and the vapor is injected through a 0.25 mm diameter needle as an effusive gas jet into the interaction region. The target density is regulated by an all-metal precision leak valve and monitored via the residual chamber pressure kept at the range of 10^{-6} Torr.

The experimental chamber is equipped with an electrostatic cylindrical mirror spectrometer [16], which selects in energy the positive ion fragments originated from the ionization of the water molecule (H_2O^{q+}). The detection of those fragments is done by an electron multiplier (channeltron) detector. By varying the homogeneous electric field created between the cylinders normalized in energy steps to the same pre-fixed collected charge, the total fragment energy distributions can be measured. The energy distribution spectra were taken in 0.5 eV steps and the acquisitions were normalized to the projectile beam current and to the residual target pressure. The intensities were corrected to the transmission function of the spectrometer (i.e. intensities divided by E/q). The spectra exclude thermal ions originated from the molecule ionization with or without dissociation, therefore single ionization was not measured with this method. The total fragment energy distributions were recorded for several angles of emission with respect to the beam direction, from 10 up to 170 degrees. Measurements were carried out for several projectiles with different charge states and impact energies, colliding on H_2O.

4. Results

We now benchmark the predictions of the present model for two cases under exploration which cover different Z_P/v regimes. Data in Fig. 3 are presented in the form of a two-dimensional map in which the detection angles of the different dissociation fragments are plotted versus their respective kinetic energy. We consider first the molecular fragmentation of water induced by 220 keV Xe^{22+} impact ($Z_P/v = 85.12$) and compare our results to the experimental data of Pešic et al. [5]. The ions in brackets (OH^+, O^+, O^{2+} and O^{3+}) indicate those fragments that are unobserved in the experiment. As stated in Ref. [5], the reported data for O^{q+} and OH^+ ions collected with very low emission energies might be affected by spurious electric fields which affect the efficiency of the spectrometer. Hence, a direct comparison is not recommended for that particular region. If we now move to larger H^+ kinetic energies, it can be seen, that the theoretical predictions for the dissociation channels for this collision system are in agreement with the reported data. Furthermore, the obtained angular dependence of the different fragmentation channels show an anisotropy that accentuates for increasing charges of the dissociating molecu-

Please cite this article in press as: N.D. Cariatore et al., Water fragmentation induced by ion impact: Fragment-ion-energy determination at different Z_P/v regimes, Nucl. Instr. Meth. B (2017), http://dx.doi.org/10.1016/j.nimb.2017.04.096

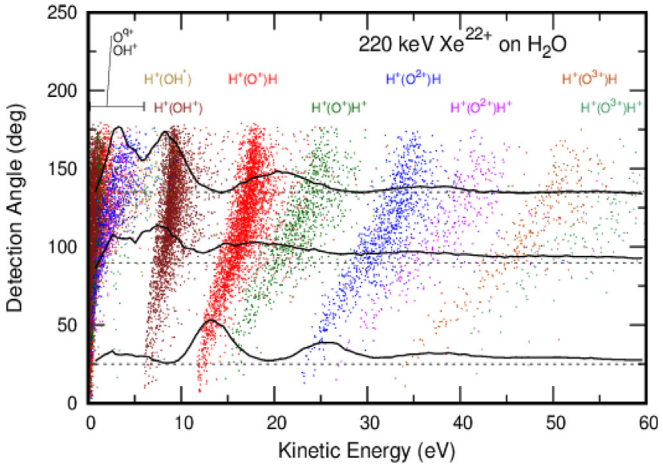

Fig. 3. Detection angle of the dissociation fragments versus their kinetic energy at 220 keV Xe^{22+} + H_2O collisions. Experimental spectra of Ref. [4] at emission angles of 25°, 90° and 135° with respect to the beam direction are explicitly shown.

lar ion. The PCI of the projectile with the different fragment also leads to the spread of events around the expected positions for the KER lines from a pure (i.e. no-projectile) CE calculation. Removal of up to 5 electrons is theoretically predicted although the number of such events is almost negligible compared to double electron removal as can be inferred from Fig. 3.

In Fig. 4 we show a similar analysis for the collision system 3 MeV Li^{3+} + H_2O (Z_P/v = 0.72). Energy distributions of the fragment ions were measured at several emission angles from 10° to 170°. As an example, Fig. 4a displays the ions energy distributions measured at emission angles of 10° and 90°, where the later distribution is divided by a factor of 2.5 to clearly highlight the angular independence of the experimental distribution in energy and intensity. Fig. 4b shows the energy centroids of the fragmentation channels as function of the observation angle predicted by the present CE calculations for the 3 MeV Li^{3+}. It can be seen from Fig. 4b that the calculated KER lines for the different dissociation channels are nearly isotropic. Moreover, events are concentrated in a set of discrete lines as expected from a pure CE calculation. These features provide evidence in this Z_P/v regime of a less relevant role of the projectile in the molecular dissociation process as expected.

Furthermore, with the aid of CE-CTMC calculation, we estimated the relative contribution of the different fragmentation channels by applying a fitting procedure of peak functions (e.g. Gaussian functions). The procedure is presented in Fig. 5a and the Gaussians are centered at the energy centroid of the H^+ fragments predicted by the present CE-CTMC model (extracted from Fig. 4b). As indicated in Fig. 5a, double ionization of fragmentation channels a–c would lie in the 5–15 eV region, triple ionization associated with channels d and e in the 15–30 eV region, fourfold

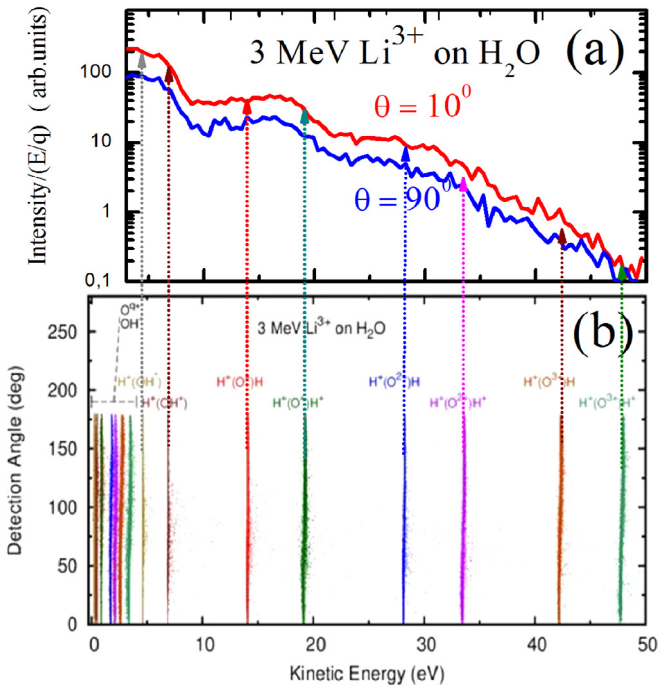

Fig. 4. Detection angle of the dissociation fragments versus their kinetic energy at 3 MeV Li^{3+} + H_2O collisions. (a) Present experimental distributions at emission angles of 10° and 90° with respect to the beam direction are explicitly shown (b) CE-CTMC model. The designation of fragmentation channels is also included.

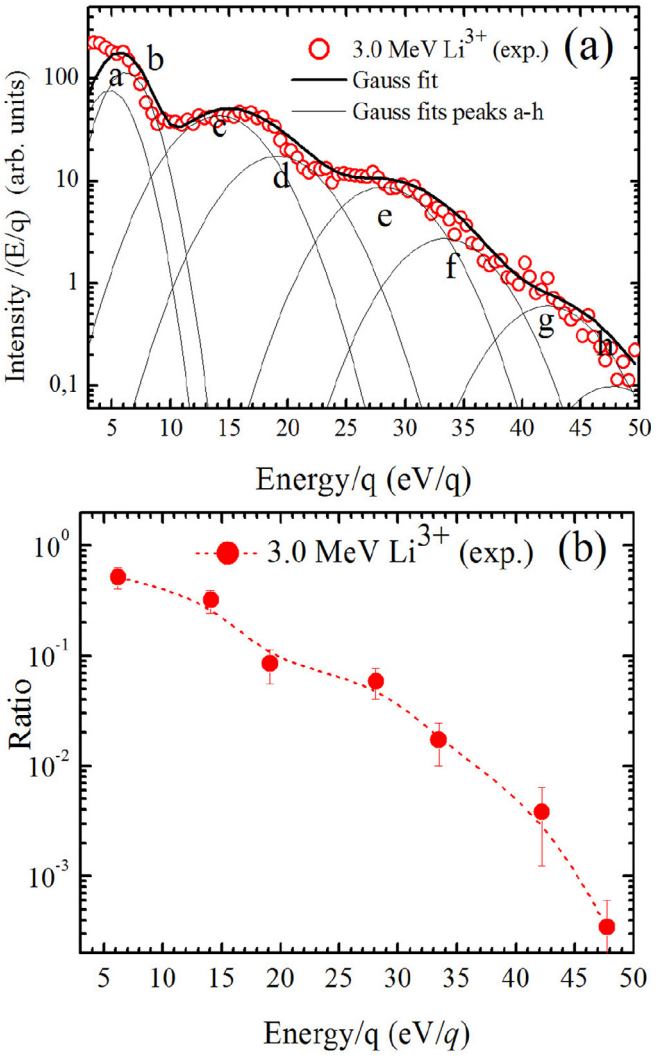

Fig. 5. (a) Relative intensities of the fragment ions as function of their energy per charge (eV/q), corrected for the transmission of the spectrometer for 3 MeV Li^{3+} at a detection angle of 10°, experimental data: red open circles, Gaussian distributions fitted to fragmentation channels (a–h) centered at the energy centroid predicted by the present CE-CTMC model: black solid lines, and black thick solid line is the sum of Gaussian distributions. (b) Ratio of fitted areas to total for each fragmentation channel at an observation angle of 10° as function of the energy centroid of the fragmentation channels: red closed circles (dotted lines to guide the eye). (For interpretation of the references to colour in this figure legend, the reader is referred to the web version of this article.)

Please cite this article in press as: N.D. Cariatore et al., Water fragmentation induced by ion impact: Fragment-ion-energy determination at different Z_P/v regimes, Nucl. Instr. Meth. B (2017), http://dx.doi.org/10.1016/j.nimb.2017.04.096

ionization associated with channels f and g in the 30–45 eV region, and fivefold ionization associated with the channel h in the 45–50 eV region. At low energies, around 2–5 eV, slow heavy fragments, mostly multiply charged oxygen ions, dominate. It was considered that the double ionization process, $H^+ + OH^+$, has a narrower distribution than the three-body distributions, namely the $H^+ + H^0 + O^{q+}$ and $H^+ + H^+ + O^{q+}$ channels, a feature that is based on the measured kinetic energies of the H^+ fragments [13]. Fig. 5b shows the ratios defined as the yield obtained from the area of the fitted functions for the fragmentation channels divided by the sum of all areas of all channels at an observation angle of 10° for 3 MeV Li^{3+} projectile as a function of the energy centroids of the fragmentation channels. It is important to note that the yield of producing energetic H^+ fragments, associated to the double, triple, 4-four and 5-fold transient charged water molecule, decreases orders of magnitude from values of 10^{-1} to 10^{-4}.

5. Conclusions

The KER spectra of fragments arising from the molecular dissociation of H_2O molecules by ion impact have been studied in a theoretical-experimental collaboration. A CE model fed event-by-event with n-CTMC simulations has been developed and successfully compared to the present data as well as to those measured for a collision system in a much larger Z_P/v regime. For the latter, the present theoretical model predicts an angular anisotropy of the KER lines for the different dissociation channels which is in general agreement with the experimental data. The mentioned anisotropy diminishes as the Z_P/v parameter decreases and the role of the projectile during the fragmentation process becomes less relevant.

More joint experimental-theoretical collaborations are needed to further improve our present understanding of the H_2O fragmentation by ion impact under general conditions. These studies would hopefully be of potential relevance for irradiation purposes in cancer-related treatments at their planning stages.

Acknowledgments

Work at IFISUR supported by Grants No. PGI 24/F059 (Universidad Nacional del Sur-(Argentina)) and No. POP 112-201101-00749 of Consejo Nacional de Investigaciones Científicas y Técnicas of Argentina (CONICET). R. S. acknowledges the support by the EU through FP7PEOPLE-2010-IRSES program 269243 DWBQS. W. W. gratefully acknowledges support from Brazilian agencies, Fundação Carlos Chagas Filho de Amparo à Pesquisa do Estado do Rio de Janeiro (Faperj), Conselho Nacional de Desenvolvimento Científico e Tecnológico (CNPq) and Coordenação de Aperfeiçoamento de Pessoal de Nível Superior (CAPES).

References

[1] M. Tarisien, L. Adoui, F. Frémont, D. Lelievre, L. Guillaume, J.-Y. Chsnel, H. Zhang, A. Dubois, D. Mathur, Sanjay Kumar, M. Krishnamurthy, A. Cassimi, J. Phys. B: At. Mol. Opt. Phys. 33 (2000) L11.
[2] J.C. Polf, K. Parodi, Phys. Today 68 (2015) 28.
[3] D. Mathur, Phys. Rep. 391 (2004) 1.
[4] C.J. Wood, R.E. Olson, Phys. Rev. A 59 (1999) 1317.
[5] Z.D. Pešic, R. Hellhammer, B. Sulik, N. Stolterfoht, J. Phys. B: At. Mol. Opt. Phys. 42 (2009) 235202.
[6] H. Ryufuku, H. Sasaki, T. Watanabe, Phys. Rev. A 21 (1980) 745.
[7] A. Bárány, G. Astner, H. Cederquist, H. Danared, S. Huldt, P. Hvelplund, A. Johnson, H. Knudsen, L. Liljeby, K.-G. Rensfelt, Nucl. Instrum. Methods B 9 (1985) 397.
[8] R. Moccia, J. Chem. Phys. 40 (1964) 2186.
[9] R.H. Garvey, C.H. Jackman, A.E.S. Green, Phys. Rev. A 12 (1975) 1144.
[10] B. Siegmann, U. Werner, H.O. Lutz, R. Mann, J. Phys. B: At. Mol. Opt. Phys. 34 (2000) L587.
[11] S. Hsie, J.H.D. Eland, Rapid Commun. Mass Spectrom. 9 (1995) 1261.
[12] Z.D. Pešic, D. Rolles, R.C. Bilodeau, I. Dimitriu, N. Berrah, Phys. Rev. A 78 (2008) 051401.
[13] F. Alvarado, R. Hoekstra, T. Schlatholter, J. Phys. B: At. Mol. Opt. Phys. 38 (2005) 4085.
[14] H. Sann, T. Jahnke, T. Havermeier, K. Kreide, C. Stuck, M. Meckel, M.S. Schoffler, N. Neumann, R. Wallauer, S. Voss, A. Czasch, O. Jagutzki, Th. Weer, H. Schmidt-Böcking, S. Miyabe, D.J. Haxton, A.E. Orel, T.N. Rescigno, R. Dörner, Phys. Rev. Lett. 106 (2011) 133001.
[15] W. Wolf, H. Luna, R. Schuch, N.D. Cariatore, S. Otranto, F. Turco, D. Fregenal, G. Bernardi, S, Suarez Phys. Rev. A 94 (2016) 022712.
[16] G. Bernardi, S. Suarez, D. Fregenal, P. Focke, W. Meckbach, Rev. Sci. Instrum. 67 (1996) 1761.

Please cite this article in press as: N.D. Cariatore et al., Water fragmentation induced by ion impact: Fragment-ion-energy determination at different Z_P/v regimes, Nucl. Instr. Meth. B (2017), http://dx.doi.org/10.1016/j.nimb.2017.04.096